Submitted to Nuclear Physics

UCRL-18925
Preprint

Cy. 2

# PERTURBED ANGULAR DISTRIBUTIONS FROM $^{120,122,124}Sn(^{40}Ar, 4n)^{156,158,160}Er$ REACTION PRODUCTS RECOILING IN VACUUM

R. Nordhagen, G. Goldring, R. M. Diamond, K. Nakai, and F. S. Stephens

August 1969

RECEIVED
LAWRENCE
RADIATION LABORATORY

OCT 16 1969

LIBRARY AND
DOCUMENTS SECTION

AEC Contract No. W-7405-eng-48

TWO-WEEK LOAN COPY

*This is a Library Circulating Copy which may be borrowed for two weeks. For a personal retention copy, call Tech. Info. Division, Ext. 5545*

LAWRENCE RADIATION LABORATORY
UNIVERSITY of CALIFORNIA BERKELEY

UCRL-18925

## DISCLAIMER

This document was prepared as an account of work sponsored by the United States Government. While this document is believed to contain correct information, neither the United States Government nor any agency thereof, nor the Regents of the University of California, nor any of their employees, makes any warranty, express or implied, or assumes any legal responsibility for the accuracy, completeness, or usefulness of any information, apparatus, product, or process disclosed, or represents that its use would not infringe privately owned rights. Reference herein to any specific commercial product, process, or service by its trade name, trademark, manufacturer, or otherwise, does not necessarily constitute or imply its endorsement, recommendation, or favoring by the United States Government or any agency thereof, or the Regents of the University of California. The views and opinions of authors expressed herein do not necessarily state or reflect those of the United States Government or any agency thereof or the Regents of the University of California.

Key Words

NUCLEAR REACTIONS: $^{120,122,124}Sn(^{40}Ar,4n)^{156,158,160}Er$, $^{150}Sm(^{20}Ne,^{20}Ne\gamma)^{150}Sm$, $E_{Ar}$ = 148 MeV, $E_{Ne}$ = 68 MeV, measured W(0°)/W(90°), W(45°)/W(90°), deduced g factors, perturbed angular distributions, time-dependent and I - J dependent hyperfine interactions, separated targets.

# PERTURBED ANGULAR DISTRIBUTIONS FROM $^{120,122,124}Sn(^{40}Ar,4n)^{156,158,160}Er$ REACTION PRODUCTS RECOILING IN VACUUM†

R. Nordhagen††, G. Goldring‡, R. M. Diamond, K. Nakai‡‡, and F. S. Stephens

Lawrence Radiation Laboratory
University of California
Berkeley, California 94720

August 1969

Abstract

Intensity ratios, W(0°)/W(90°), have been measured for γ-rays emitted from products of $^{120,122,124}Sn(^{40}Ar,4n)^{156,158,160}Er$ reactions recoiling into either vacuum or lead. The g factors for levels in the ground bands (with spins up to 8) of the Er nuclei are evaluated. The perturbation of the angular distribution due to time-dependent hyperfine interactions in highly excited, free ions was found to be strongly dependent on the nuclear spin I and the atomic spin J. The average g factor for the three Er-nuclei ground bands was found to be between 0.34 and 0.40 depending on assumed models of the I and J dependence. No large difference in g factors among the nuclei was found, although a small increase (∿ 20%) between $^{160}Er$ and $^{156}Er$ seems indicated.

†Work performed under the auspices of the U. S. Atomic Energy Commission.

††On leave from the Physics Institute, University of Oslo, Oslo, Norway.

‡On leave from the Weizmann Institute, Rehovoth, Israel.

‡‡On leave from Osaka University, Osaka, Japan.

## 1. Introduction

Hyperfine interactions, mainly in solids and liquids, have found widespread use in experimental studies both of the interactions themselves and of the magnetic and electric moments of nuclei. Among the strongest hyperfine fields encountered to date have been the magnetic fields found in highly excited, free atoms. Such atoms are produced in nuclear reactions when the bombarding energies are sufficient to let the products leave the target and recoil into vacuum or gas. Ben Zvi et al.[1]) have recently shown the occurrence of strongly perturbed gamma-ray angular distributions following Coulomb excitation of the first $2^+$ level in thin targets of even-even nuclei. By studying recoils both into vacuum and into gas the nature of the hyperfine fields was explored, and the feasibility of measuring magnetic moments of excited nuclear states by these methods was established. It was found that the time-integrated perturbation factors, $G_k$, in the angular distribution

$$W(\theta) = \sum_{k=0}^{k=2n} A_k G_k P_k(\cos\theta) \qquad (1)$$

followed the assumptions of a randomly oriented time-dependent magnetic hyperfine interaction[1]). These results, obtained with $^{16}O$ beams up to 40 MeV in energy, indicated fields of between 20 and 30 MG. The physical picture envisioned is that of a highly stripped and excited recoiling ion undergoing rapid optical transitions, and with the magnetic field at the nucleus changing randomly in direction with a correlation time, $\tau_c$, short ($\sim$ 3 ps) compared to the nuclear lifetime. The $G_k$ are given by the

theory of Abragam and Pound[2]) as

$$G_k = \frac{1}{1 + \lambda_k \tau_m} \tag{2}$$

with $\tau_m$ as the mean nuclear lifetime and

$$\lambda_k = p_k \omega^2 \tau_c \tag{3}$$

where $p_k = \frac{1}{3} k(k+1)$ and $\omega = g \frac{H\mu_N}{\hbar}$ is the Larmor frequency with $g$ as the nuclear g factor. Thus the perturbation depends on the $g$ factor, the field strength, and the two times involved.

In the present work, strongly perturbed angular correlations have been studied following heavy-ion compound-nucleus reactions of the type (HI,xn). In the specific reactions chosen, $^{120,122,124}Sn(^{40}Ar,4n)^{156,158,160}Er$, the recoil velocities of the product nuclei are of the order of 2% the speed of light for a bombarding energy of 150 MeV. Thus large hyperfine fields are expected when the product nuclei recoil in vacuum.

The compound nucleus itself is initially formed in a state of high excitation and high spin (40 - 50 $\hbar$ in these cases), and after neutron emission spends a considerable time in the "yrast" cascade, passing down through the states of highest possible angular momentum with the lowest energies[3]). When members of the ground-state band become the lowest-lying levels with high spin, the decay cascade enters that band. The succeeding transitions in the ground band are observed as distinct gamma-ray peaks superimposed on a generally smooth background of the numerous high-lying transitions.

For bombarding ions as heavy as $^{40}Ar$ almost all the independent feeding of the ground-band is to the highest two or three states observed. In the nuclei studied the spin of these highest states varies from $\sim 10$ in $^{156}Er$ to $\sim 14$ in $^{160}Er$. Most importantly, the feeding time before the band is entered varies from $16 \pm 3$ ps in the vibrator $^{156}Er$, through $11 \pm 3$ ps for $^{158}Er$, to $6 \pm 3$ ps in the rotor $^{160}Er$[4]).

The nuclei are initially highly aligned with the beam direction, and a pronounced angular distribution of the decay gamma rays is expected[5]). Although some spreading of the initial $m = 0$ substate population is observed, sufficient alignment persists to give a ratio of the 0° to 90° gamma-ray intensities, $W(0°)/W(90°)$, near 1.5 in the present cases. This ratio for an ideal, high-spin $m = 0$ substate population is close to 1.6.

In most angular distribution experiments one tries to observe the unperturbed gamma-ray intensities from nuclei recoiling into metal backings, in our cases, lead. For the relatively long-lived states (well above 100 ps) perturbations may, occur also with these targets, as will be discussed. Perturbations of the short-lived states, for instance due to transient perturbations may occur also with these targets, as will be discussed appreciable in the present measurements and we regard the results on short-lived states from lead-backed targets as unperturbed. Deviations from ideal alignment are then attributed to the spreading of the initial population.

The aim, then, of the present experiments is to observe both unperturbed and perturbed distributions for the gamma-ray transitions involved in the

decay of the ground-band states of the three erbium nuclei. These nuclei were chosen because information on ground-band systematics and life times are available from previous studies[4,6]). The objective was then to extract g factors from the measured distributions and thus study the magnetic properties of excited states of the nuclei.

## 2. Experimental Methods

The following three sets of experiments were performed. First, thin targets (1 mg/cm$^2$) of the separated isotopes $^{120,122,124}$Sn on thick lead backings were bombarded with $^{40}$Ar in order to observe the unperturbed intensities. Secondly, thin, self-supporting targets of the same thickness were used to measure the perturbed intensities for the reaction products recoiling into vacuum. Thirdly, the gamma-ray anisotropies following Coulomb excitation of $^{150}$Sm by $^{20}$Ne both on lead-backed and self-supporting targets (approx. 1 mg/cm$^2$), were observed. As the g factor of $^{150}$Sm was determined by Ben Zvi et al.[1]), this last experiment effectively determines the field at higher recoil velocities.

In all cases heavy-ion beams from the Lawrence Radiation Laboratory HILAC accelerator were used. These were pulsed with a duty cycle of $\sim$ 20%. The beam energy for the ($^{40}$Ar,4n) reaction was 148 MeV, and for the Coulomb excitation, 68 MeV $^{20}$Ne ions were used.

For each target studied with the ($^{40}$Ar,4n) reaction, two gamma-ray spectra were observed simultaneously, one from a Ge(Li) counter situated at 0° to the beam direction, and one from a second Ge(Li) counter at 90°. The spectra were each accumulated in 2048 channels of the HILAC PDP-7 computer installation. The counter gamma-ray pulses were fed to two fast

successive-approximation ADC's[7]) via the standard Berkeley high-resolution high counting-rate amplifying system consisting of a preamplifier, linear amplifier, pile-up rejector and linear gate. The ADC's were gated on only during beam bursts, and derandomizers were inserted between the linear gates and the ADC inputs to accommodate the high in-beam counting rates ($\sim$ 15000 c/s).

Dead time was determined in the following manner. Two pulse generators were set to feed each of the counter preamplifiers, respectively. These pulses were counted as 'totals'. The pulses, suitably delayed, were also brought into coincidence with the output pulses from the pile-up rejector. These coincident pulses were counted as 'valids', and the ratio of valids to totals gave the true live time through the pile-up rejector. To get a sampling depending on the instantaneous beam rate, each pulse generator was triggered by pulses from the other counter. To avoid pulse overlap and additional cross talk, the pulses were first scaled down by a factor of 50 or 100, and were delayed for 50 μs before triggering the opposite pulser. As the peak due to the pulsers also could be made to appear in the γ-ray spectra, the integrated pulser yield in a spectrum relative to the totals would give the live time including the effect of the derandomizer and ADC. At the counting rates used, the principal dead time was due to the pile-up rejector which normally was set to reject pulses closer than 12 μs apart.

Further complications arose from the fact that the two Ge(Li) counters were not identical, having front face areas times drift depths of 7 $cm^2 \times 0.9$ cm and 5 $cm^2 \times 1.3$ cm, respectively. Furthermore, as the overall counting rates at 0° and 90° to the beam differed by 50%, the counter to target distances were set differently to equalize the counting rates in the two counters.

These distances were approx. 4.5 cm, and the counters were covered with 400 mg/cm$^2$ silver absorbers. To obtain the true ratio of 0° to 90° yields, the counter efficiencies were carefully measured with a radioactive source of $^{177m}$Lu, placed in the target position with the source deposit in the beam-spot center. The target chamber itself was a circular aluminium cylinder of 5 cm diameter. The beam was collimated down to a size of approx. 6 × 3 mm, and the targets were mounted at 45° to the beam direction. During a series of runs, the anisotropy of the high-yield Coulomb excitation in a thick foil of Ta was measured at regular intervals. Thus any change in anisotropy due to beam movement could be detected. Within one series of runs, the change was negligible, but the Ta anisotropies provided a convenient normalization between series taken at different times.

The more long-lived recoils had mean travel distances in vacuum of up to 8 mm[4]). To confine these recoils to the chamber center, thin lead foils were mounted 1.5 mm behind the thin targets. As the linear momentum of the product recoils are in the direction of the beam, the 0° counter observes strongly Doppler-shifted γ-rays from recoils decaying in flight. The recoils actually being stopped in the lead foils give rise to unshifted γ-rays and the ratio of shifted to unshifted intensities can be found. If we denote this ratio as R, the mean distance of decay for the recoils is found to be $d = \frac{R}{1+R}\,\delta$, where $\delta$ is the travel distance corresponding to the mean life of the decaying state. The counter solid angles have to be corrected for this distance.

In the case of the Coulomb excitation of $^{150}$Sm, the γ-rays from the 334 keV transition was observed in backscatter coincidence with the $^{20}$Ne ions.

Two 5 cm by 5 cm NaI(Tl) counters were used at 11 cm from the target, and the backscatter particle counter had a mean angle of 160° to the beam direction. The coincidence events were accumulated on magnetic tape by the PDP-7 multi-dimensional hardware as two γ-ray spectra, one particle spectrum and a time spectrum. The coincidences were detected with a standard fast-slow system involving a time-to-height converter. The two counters were situated at 45° and 90° to the beam, respectively. Finally, the coincidence spectra were obtained by sorting the accumulated events as to backscatter particle peak and time-spectrum peak, after correcting for separately sorted random events.

## 3. Results

### 3.1. INTENSITY RATIOS

Representative gamma-ray spectra are shown in fig. 1 for the $^{122}Sn(^{40}Ar,4n)^{158}Er$ reaction at 90°, both on lead-backed and self-supporting targets. In the latter case the γ-ray peaks are broadened due to the Doppler shift. The actual γ-ray yields were obtained by analyzing the spectra with the peak-fitting program written for the Berkeley CDC 6600 by Routti and Prussin[8]). The peak intensities were corrected for the changes in solid angle with recoil distance and for the relative peak efficiency of the two counters. Also, an efficiency correction due to the increase in γ-ray energy caused by the Doppler shift at 0° was considered. However, it is found that this decrease in efficiency is almost compensated for by the relativistic increase due to decays in flight. Finally, for each transition the intensity ratio was obtained as the ratio of peak yields at 0° and 90°, W(0°)/W(90°).

Due to the difference in counter size, the relative efficiency as a function of γ-ray energy varied strongly from around 130 keV on down. Thus, the intensity ratio for the 2 → 0, 126.2 keV transition in $^{160}$Er was difficult to obtain. Moreover, this long-lived ($\tau_m$ = 1.3 ns) transition was almost totally perturbed already in the lead-backed target, presumably due to magnetic interactions from hyperfine fields of Er in Pb. Therefore as the unperturbed intensity ratio could not be established, the transition was excluded from further analysis. Also a slight perturbation of the 2 → 0, 192.7 keV transition in $^{158}$Er ($\tau_m$ = 0.43 ns) was observed from lead-backed targets, but in this case we used as the unperturbed intensity ratio the value obtained from the faster transitions in $^{158}$Er. For the self-supporting targets, the Doppler broadening and the quality of the spectra made the extraction of yields from peaks above approx. 500 keV less meaningful, and perturbed intensity ratios above this energy were therefore not obtained. The final intensity ratios are listed in table 1, together with the nuclear properties of the excited states.

For the $^{150}$Sm yields, the intensity ratios for the 334 keV peak in the 45° and 90° coincidence spectra are given in table 2, both for lead-backed and for self-supporting targets.

### 3.2. PERTURBATION FACTORS

The unperturbed theoretical angular distributions contain the two terms with k = 2 and 4

$$W(\theta) = 1 + A_2Q_2P_2(\cos\theta) + A_4Q_4P_4(\cos\theta) \quad . \tag{4}$$

To analyze the influence of a perturbing interaction in the present case, where only the one ratio $W(0°)/W(90°)$ is observed, an explicit relationship between the two terms must be assumed. The quantities $Q_2$ and $Q_4$ are the tabulated[9]) angular-distribution attenuation coefficients due to the finite solid angle of the detectors. The $A_2$ and $A_4$ are the theoretical angular-distribution coefficients where, for the analysis of the ($^{40}$Ar,xn) results, we use the formalism and tables of Yamazaki[10]). For complete alignment of the initial states the stretched cascade should show an intensity ratio (0°/90°) of 1.64 (with $Q_2 = 0.95$, $Q_4 = 0.85$). The mean unperturbed ratio for the short-lived states is observed to be 1.47 ± 0.02. We attribute this difference as due to the Gaussian spreading of the initial alignment, and assume the spreading to be represented by the coefficients $\alpha_2$ and $\alpha_4$;

$$W(\theta) = 1 + A_2\alpha_2Q_2P_2(\cos\theta) + A_4\alpha_4Q_4P_4(\cos\theta) = 1 + b_2P_2 + b_4P_4 \qquad (5)$$

where the relationship between $\alpha_2$ and $\alpha_4$ is given by Yamazaki (formulas (10), (11), and fig. 2, Ref. 10). For instance, the average intensity ratio 1.47 gives values of $b_2 = A_2\alpha_2Q_2$ and $b_4 = A_4\alpha_4Q_4$ of 0.28 and -0.05, respectively. Taking the perturbed angular distribution as

$$W(\theta) = 1 + G_2b_2P_2(\cos\theta) + G_4b_4P_4(\cos\theta) \qquad (6)$$

we again need a relationship between the factors with $k = 2$ and $k = 4$ to extract a measure of the perturbation. As the hyperfine interaction was originally found to be of a simple time-dependent magnetic-dipole character[1]), we will explicitly assume the relationship

$$G_4 = 3G_2/(10-7\ G_2) \tag{7}$$

which is valid for this interaction. As will be discussed later, the perturbation factors may depend on other properties of the system, and so the above relationship may only be an approximation. However, as the $k = 4$ terms are small in all cases, the errors introduced will be negligible. By using the perturbed anisotropies, the values of $b_2$ and $b_4$ obtained from the unperturbed anisotropies, and the $G_4$ relationship, we find the values of $G_2$ given in table 1 as the final measure of the perturbation.

In the case of the $^{150}$Sm distributions, the theoretical, unperturbed value of $W(45°)/W(90°)$ was estimated by using the Winther-de Boer multiple Coulomb excitation program[11]). Taking the feeding from higher states into account, this intensity ratio for the 334 keV transition was calculated to be 6.8. This was close enough to the observed unperturbed value to permit the use of the ratio of calculated $b_2$ and $b_4$ together with the measured unperturbed and perturbed anisotropies, and the $G_4$ relationship, to find the $G_2$ value listed in table 2.

In figs. 2 and 3 the values of $G_2$ are shown as a function of mean lives for the different transitions excited in the Er nuclei. These values (last column in table 1) are obtained by assuming that the unperturbed intensity ratio in each reaction is the average value observed with the lead-backed targets for the transitions with a mean life less than 0.1 ns. To give an impression of the quality of the data, $G_2$ values obtained for each of the unperturbed transitions are also included on the figures.

## 4. Analysis and Discussion

### 4.1. THE TIME-DEPENDENT INTERACTION

For a magnetic dipole interaction, in the case of a simple time-dependent, randomly fluctuating hyperfine field, the perturbation factor is

$$G_2 = 1/(1 + 2\omega^2\tau_c\tau_m) \quad . \tag{8}$$

In the following it will be explicitly assumed that the $g$ factor for the excited states within one ground band stays constant, as is expected in a rotational nucleus. With this approximation, to be discussed later, the experimental $G_2$ values are fitted with the above equation. For each nucleus then, one value of $\omega^2\tau_c$ is obtained. To extract a $g$ factor from these $\omega^2\tau_c$ values, $H^2\tau_c$ for the Er case is computed from $\omega^2\tau_c$ from the $^{150}$Sm case using a $g$ factor of $0.32 \pm 0.02$[1]) for $^{150}$Sm. We have corrected the Sm field 2% for the change in $Z$ based on interpolation between measured values in Sm and Yb at lower velocities, and have made an additional 6% correction for the difference in velocity, using the best presently available relationship[12]), $H \propto v^{0.6}$. Thus, the field value for the Er case, obtained with the same correlation time, $\tau_c = 3$ ps, as in ref. 1, is $41 \pm 7$ MG.

If the simple time-dependent theory is assumed, the perturbation takes place during the entire decay cascade, the yrast region included. In this case, the fits shown in fig. 2 and given as case 1, table 3 are obtained. As can be seen the fits are poor and $\chi^2$ is large. Moreover, the average $g$ facotr obtained, $g = 0.24$, is considerably smaller than the value of $g_R$ found in this mass region, $g_R \sim 0.03$. The fit is relatively sensitive to the value

of g; taking g as 0.3, for example, gives a $\chi^2$ of 11. Thus, it seems that the assumptions of a constant g factor or a full perturbation during the entire decay are not in accord with the observations.

If on the other hand, it is assumed that the perturbation only takes place in the ground band, the fit is considerably improved (case 2, table 3, $\chi^2 \sim 2$, average $g \sim 0.34$). Clearly then, a possible explanation is that the perturbation is markedly reduced for the higher states, either due to their magnetic properties or due to their high nuclear spins. For instance, a vanishingly small g factor for the high-lying states in the yrast region will perfectly well explain the data. However, it has not been found possible to construct a sensible model for these states where the g factor is so strongly reduced. A more plausible explanation is that the high spin of the states is responsible for the reduction, and that the time-dependent theory must be modified accordingly.

## 4.2. THE I AND J DEPENDENCE

The perturbation from a hyperfine interaction in a free atom is due to the precession of the nuclear spin I around the total atomic spin F. In the free atom, I and the spin J of the electron configuration couple to the resultant F. When I is large and J small, I is highly aligned with F and the change in orientation of I with precession is small (the static perturbation). Furthermore, a change in direction and magnitude of a small J, e.g., due to optical transitions, will not change the direction of F in space appreciably. Thus the influence on the orientation of I from a changing J is also small (the time-dependent perturbation). Only when J has a magnitude comparable to or greater than I will large perturbations

occur. This is in contrast to the usual case where a field establishes a reference axis outside the atom, and no I and J dependence of the interaction is expected[13]).

The dependence of the interaction on I and J will introduce a correction factor in the expression for $G_k$ given in eq. (2). Using a simple time dependent model (discussed below) we have shown that this correction factor, K(I,J), enters the expression for $G_k$ as follows:

$$G_k(I,J) = [1 + p_k\omega^2\tau \cdot \tau_c K(I,J)]^{-1} \quad . \tag{9}$$

In fact, it seems plausible that the correction will, in general, enter in this way, though we have not been able to show this. In the following discussion we will assume the form of eq. (9) for $G_k(I,J)$ and examine several simple possibilities for K(I,J). Results of analyzing the data based on these possibilities are summarized in table 3.

One of the simplest forms for K(I,J) is obtained with the assumption of no perturbation for $J \leq I$, i.e., K(I,J) = 0, and the full perturbation for $J \geqslant I$, i.e., K(I,J) = 1. In this case the best fit to the data is with an effective cut-off at I = 8, and the result is presented as case 3 in table 3. Perhaps a more realistic estimate for K(I,J) is to make use of calculations for static interactions in free atoms. This case has been considered by Alder[13]), who found an I and J dependence of the type under discussion. From these calculations we can estimate K(I,J) for use in the present time-dependent case. We find that K(I,J) is mainly a function of the ratio, I/J, and the actual values obtained are plotted in fig. 4, curve A. The best fit

to the data using this curve for $K(I,J)$ is very close to the one obtained for case 4a, table 3, and shown in fig. 3.

We have also set up a simple time dependent model to evaluate $K(I,J)$. The main assumptions are: a) a cut-off of the hyperfine interaction above a certain value of $I$; b) a time-independent average distribution for $J$; and c) a random-walk for changing $J$. The detailed results depend largely on the relationships among the nuclear lifetime, the time required for a step in the random-walk process, and an effective correlation time, which is the time to make a significant change in the field direction. Under the assumption that the effective correlation time is short compared to the time required to run through the entire $J$ distribution, and that both of these are short compared to the nuclear lifetime, we get:

$$K(I,J_o) = 1/2\, e^{-I/J_o} \left[(I/J_o)^2 + 2(I/J_o) + 2\right] ,$$

where $J_o$ is the mean value of an assumed exponential $J$ distribution. This expression for $K(I,J)$ is also plotted in fig. 4 as curve B, and the fits to the data for three $J_o$ values are given as case 4 in table 3. If the effective correlation time is comparable with the time required to run through the $J$ distribution, then:

$$K(I,J_o) = e^{-2I/J_o} .$$

The best fit for this case is also given in table 3, case 5.

From table 3 it is clear that when $\chi^2$ is reasonable, very similar values for the $g$ factors are obtained. This is nearly independent of the

actual form of $K(I,J)$; even the simple cut-off gives values close to the ones for the more elaborate models. In fact, a detailed interpretation of the $I$ and $J$ dependence is difficult, mainly because of lack of information on the de-excitation process (e.g. the $J$ distribution) in free, highly-ionized atoms. However, the general behavior of $K(I,J)$ is expected to be as shown on fig. 4.

## 4.3. THE g FACTORS

The biggest uncertainty in the measurement of $g$ factors by recoil into vacuum is the aging of the ionic population and the resulting time dependence of the ionic parameters. The experimental evidence of previous work as well as the present study suggest that the important parameter $H^2\tau_c$ does not change very much; at most some 50 percent in $3 \times 10^{-10}$s. The possible variation of $H^2\tau_c$ with time is nevertheless a substantial handicap in measurements of $g$ factors of states with widely different mean lives. In the present measurement this difficulty is avoided by averaging the $g$ factors of each isotope over several levels. Only these averages, involving broadly overlapping time regions, are compared among the three isotopes.

The $g$ factors obtained under the various assumptions are summarized in table 3. As pointed out previously, the average $g$ factor is reasonably independent of the particular model used, provided $\chi^2$ is small. We take case 4a as a representative value, with $g = 0.37 \pm 0.03$ as the average. The uncertainty in this value, both due to the statistics and due to the systematic error introduced by not knowing the exact $I - J$ dependence, makes the drawing of exact conclusions difficult. However, an average $g$ factor of 0.37 is close to the ones observed for the heavier Er nuclei ($0.33 \pm 0.01$ in $^{168}$Er [14]), $0.32 \pm 0.01$ in $^{166}$Er [14,15]), and $0.35 \pm 0.01$ in $^{164}$Er [16])).

Of more significance may be the fact that the separate $g$ factors found for the three Er nuclei are nearly the same (within 20%). For other nuclei in the region of neutron numbers $N = 88$ to 92 there are large variations in the measured $g$ factors of the $2^+$ states which are not understood at present.

No ¶

The small differences observed in the present study may indicate an increasing $g$ factor with decreasing mass number, but this trend may not be statistically significant.

The data further suggest that there are no significant differences in the $g$ factors for the different excited states within the ground bands. This is one of the implicit assumptions of the analysis, however, so the apparent constancy of the $g$ factor may not be real. Since we explicitly assume an $I$ dependence of the perturbation, a change in $g$ factor within a band may be masked by the change in hyperfine interaction with $I$. On the other hand, as states with the same $I$ in the different bands have widely different mean lives, the change in $g$ factor with $I$ must be correlated with mean life to produce such a masking. It is therefore probable that the change in $g$ factor among the levels within the ground bands is not large.

To conclude then, we have found evidence that a strong $I$ and $J$ dependence does occur in the hyperfine perturbation of angular distributions from highly excited ions, an effect which has not previously been observed. It is still possible to obtain information on $g$ factors from the perturbed distribution, provided the effect is taken into account. However, detailed information can not be obtained until more is known about the atomic processes involved, and on how the perturbation is influenced by the variation both in magnitude and direction of the atomic spin $J$.

If I is large,

And J is small,

Then I can't be

Perturbed at all.

Acknowledgments

We are particularly indebted to Z. Vager for suggesting the idea of an I-dependent hyperfine interaction. Discussions with D. Quitmann and D. A. Shirley are also gratefully acknowledged. The help of L. B. Robinson and D. Landis with the electronic systems and the HILAC staff with running the experiments, is highly appreciated. One of us (R.N.) is grateful for a grant from the Royal Norwegian Council for Scientific and Industrial Research.

## References


1. I. Ben Zvi, P. Gilad, M. Goldberg, G. Goldring, A. Schwartzschild, A. Sprinzak, and Z. Vager, Nucl. Phys. A121 (1968) 592
2. A. Abragam and R. V. Pound, Phys. Rev. 92 (1953) 943
3. J. O. Newton, F. S. Stephens, R. M. Diamond, W. H. Kelly, and D. Ward, University of California Lawrence Radiation Laboratory Report UCRL-18348, to be published
4. R. M. Diamond, F. S. Stephens, W. H. Kelly, and D. Ward, Phys. Rev. Letters 22 (1969) 546
5. J. O. Newton, F. S. Stephens, R. M. Diamond, K. Kotajima, and E. Matthias, Nucl. Phys. A95 (1967) 357
6. D. Ward, F. S. Stephens, and J. O. Newton, Phys. Rev. Letters 19 (1967) 1247
7. L. B. Robinson, F. Gin, and F. S. Goulding, Nucl. Instr. Methods 62 (1968) 237
8. J. T. Routti and S. G. Prussin, University of California Lawrence Radiation Laboratory Report UCRL-17672, to be published
9. J. Black and W. Gruhle, Nucl. Instr. Methods 46 (1967) 213; M. J. L. Yates in "Alpha, Beta and Gamma-Ray Spectroscopy", ed. K. Siegbahn (North Holland Publishing Co., Amsterdam, 1965) 1691
10. T. Yamazaki, Nucl. Data 3A (1967) 1
11. A. Winther and J. de Boer, in "Coulomb Excitation", a collection of reprints (Academic Press, New York-London, 1966) 303
12. G. Goldring, Proceedings of the International Conference on Properties of Nuclear States, Montreal, 1969, (to be published).

13. K. Alder, Helv. Phys. Acta 25 (1952) 235

14. E. Münck, D. Quitmann, and S. Hüfner, Z. Naturf. 21a (1966) 847

15. H. Dobler, G. Petrich, S. Hüfner, P. Kienle, W. Wiedemann, and H. Eichler, Phys. Letters 10 (1964) 319

16. E. Münck, S. Hüfner, and D. Quitmann, Phys. Letters 24B (1967) 392

Table 1

Intensity ratios and perturbation factors for erbium nuclei recoiling in vacuum.

| Er nuclide mass no. | Transition | $E_\gamma$ kev | Mean[a] life, ps | W(0°)/W(90°) from Lead backed target: | Self supporting target: | $G_2$ [b] |
|---|---|---|---|---|---|---|
| 156 | 2-0 | 399.4 | 47.9 | 1.51 ± 0.03 | 1.11 ± 0.02 | 0.23 ± 0.04 |
| | 4-2 | 452.9 | 7.83 | 1.50 ± 0.03 | 1.37 ± 0.04 | 0.73 ± 0.08 |
| | 6-4 | 543.2 | 1.65 | 1.56 ± 0.05 | --- | --- |
| | Unperturbed Average | | | 1.52 ± 0.02 | | |
| 158 | 2-0 | 192.7 | 433. | 1.39 ± 0.02[c] | 1.03 ± 0.02 | 0.07 ± 0.05 |
| | 4-2 | 355.7 | 20.8 | 1.47 ± 0.03 | 1.22 ± 0.02 | 0.47 ± 0.04 |
| | 6-4 | 433.8 | 4.04 | 1.51 ± 0.04 | 1.46 ± 0.04 | 0.93 ± 0.08 |
| | 8-6 | 523.8 | 1.75 | 1.58 ± 0.06 | --- | --- |
| | Unperturbed Average | | | 1.49 ± 0.02 | | |
| 160 | 2-0 | 126.2 | 1330. | 1.12 ± 0.02[c] | [d] | [d] |
| | 4-2 | 264.3 | 49.8 | 1.42 ± 0.02 | 1.13 ± 0.02 | 0.31 ± 0.05 |
| | 6-4 | 376.3 | 7.77 | 1.42 ± 0.03 | 1.35 ± 0.02 | 0.82 ± 0.05 |
| | 8-6 | 464.6 | 3.12 | 1.47 ± 0.03 | 1.46 ± 0.04 | 1.08 ± 0.09 |
| | 10-8 | 532.1 | 1.79 | 1.46 ± 0.04 | --- | --- |
| | Unperturbed Average | | | 1.43 ± 0.02 | | |

[a])From Diamond *et al.*[4]).

[b])$G_2$ taken relative to the average unperturbed anisotropy from each lead-backed target.

[c])Perturbed possibly due to magnetic interaction of Er in Pb. Not included in unperturbed average.

[d])Not included in the analysis. The transition energy made the establishment of true anisotropy difficult, and the long life of the state will in any case give complete perturbation.

Table 2

Intensity ratios (W(45°)/W(90°)) and perturbation factors for the Coulomb excitation of $^{150}Sm$ with $^{20}Ne$ at 68 MeV, 334.0 keV 2 → 0 transition.

| | | |
|---|---|---|
| W(45°)/W(90°) from lead backed target | : | 6.5 ± 0.3 |
| " from thin target | : | 1.44 ± 0.04 |
| Expected full intensity ratio, feeding from higher states and geometry corrections taken into account | : | 6.8 |
| $G_2$ attenuation factor from experimental anisotropies | | 0.41 ± 0.03 |
| $\omega^2\tau_c$ | : | $(1.0 \pm 0.1) \times 10^{10} s^{-1}$ [a] |
| Assumed g-factor from ref. 1 | : | 0.32 ± 0.02 |
| Hyperfine field | : | 38 ± 7 MG [ab] |
| Average recoil energy of Sm nuclei | : | 23 MeV |

[a] Without the I-J dependence.

[b] $\tau_c = 3 \pm 1$ ps[1].

Table 3

Values of $\omega^2\tau_c$ and $\chi^2$ for fits to $G_2$ versus $\tau_m$ under different assumptions.

| Case | Assumption | $\chi^2$ | Average $\omega^2\tau_c \times 10^{10}$ [a]) | Average g factor[a]) | Separate nuclei[b]) 156 g[a]) | 158 g[a]) | 160 g[a]) | Figure |
|---|---|---|---|---|---|---|---|---|
| 1 | Simple time dependence, full perturbation in yrast region | 4.6 | 0.8 ± 0.2 | 0.24 ± 0.02 | 0.26 | 0.25 | 0.21 | 2 |
| 2 | Simple time dependence, perturbation in ground band only | 2.0 | 1.4 ± 0.2 | 0.34 ± 0.02 | 0.40 | 0.34 | 0.26 | |
| 3 | I-J dependence by cutoff for I > J, J = 8 | 1.5 | 1.5 ± 0.2 | 0.36 ± 0.03 | 0.40 | 0.36 | 0.31 | like 3 |
| 4a | I-J dependence as curve B, fig. 4, $J_o = 3$ | 1.6 | 1.7 ± 0.3 | 0.37 ± 0.03 | 0.39 | 0.37 | 0.34 | 3 |
| b | $J_o = 6$ | 4 | 5.8 ± 1.0 | 0.63 ± 0.05 | | | | |
| c | $J_o = 1$ | 3 | 0.8 ± 0.2 | 0.28 ± 0.03 | | | | |
| 5 | I-J dependence as $\exp(-2I/J_o)$, $J_o = 12$ | 1.8 | 1.9 ± 0.3 | 0.40 ± 0.03 | 0.42 | 0.39 | 0.39 | |

[a])Obtained with $H^2\tau_c = (1.16 \times (H^2\tau_c)_{Sm})$, at an Er recoil energy of 28 MeV. Ref. Sect. 4.1. Cases 4 and 5 corrected for K(I,J) of the $I=2^+$ state $^{150}Sm$. (Case 4a, 0.97; Case 5, 0.72) Case 4a taken as a representative average.

[b])Individual errors approx. 15%.

Figure Captions

Fig. 1. Typical gamma-ray spectra from a Sn($^{40}$Ar,4n)Er reaction, observed with 6.3 cm$^3$ Ge(Li) detectors at 4.5 cm from the target.

Fig. 2. Perturbation factors, $G_2$, for transitions in the ground bands of $^{156,158,160}$Er recoiling in lead and in vacuum, plotted against the mean life of the emitting level. The lines are drawn through the calculated points only, and do not give the variation of perturbation with mean life, as this depends on the mean lives of the previous transitions in the cascade. The fit is performed under the assumption of a full perturbation taking place during the entire decay cascade, including the yrast region.

Fig. 3. Perturbation factors, $G_2$, for transitions in the ground bands of $^{156,158,160}$Er recoiling in lead and in vacuum, as in fig. 2 but for the assumption of an I-J dependent perturbation (case 4a, table 3). The lines drawn through the calculated points have the same significance as in fig. 2.

Fig. 4. The effective reduction of the perturbation for different cases of I-J dependence. A: The effective decrease in the hard-core perturbation for a free atom[13]) compared with the hard-core value for a randomly oriented, static field. B: An example of a possible K(I,J) variation in a time-dependent case (case 4, table 3). In this case J represents the mean value, $J_o$, of the J distribution.

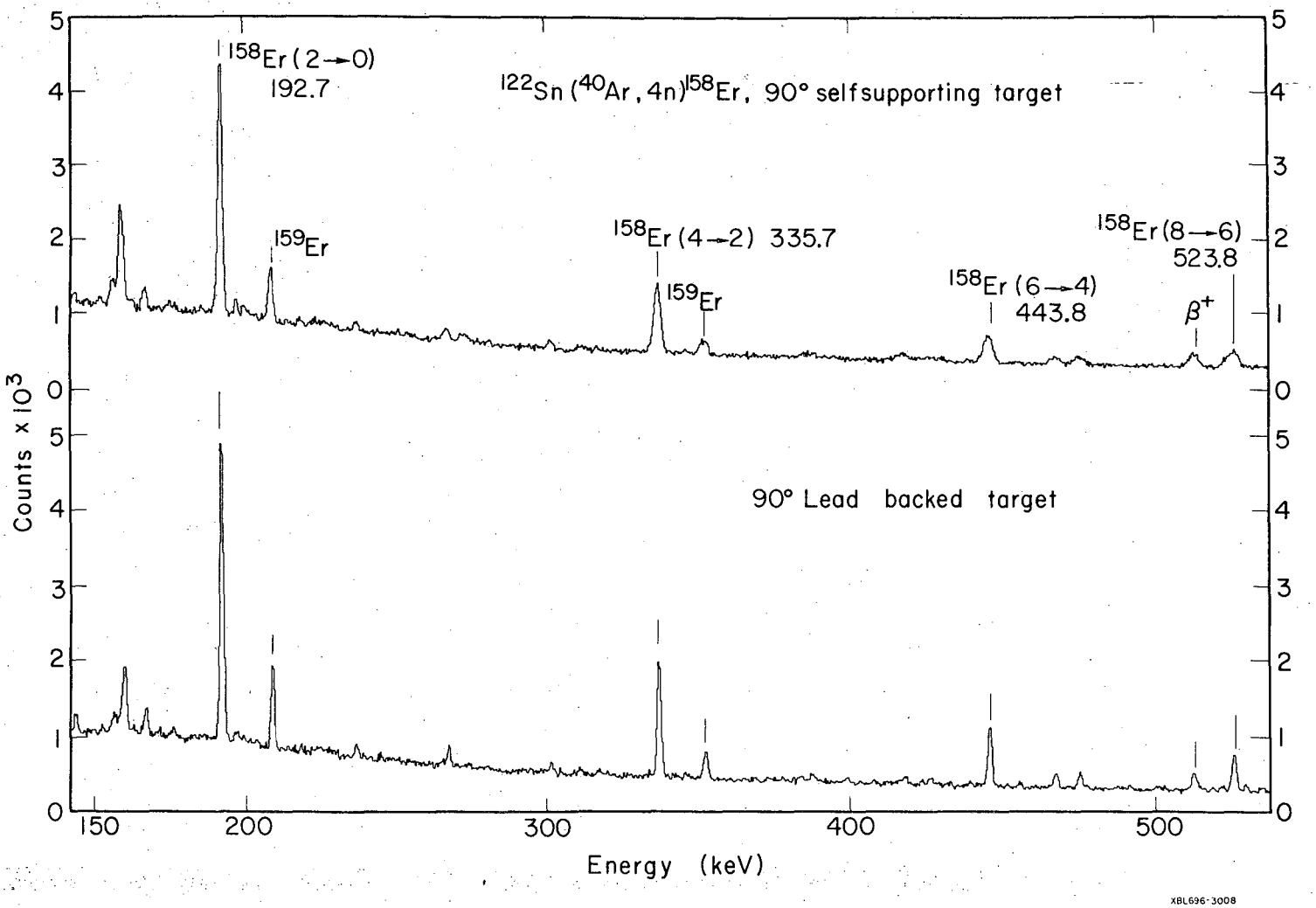
$^{158}$Er (2→0)
192.7
$^{122}$Sn ($^{40}$Ar, 4n)$^{158}$Er, 90° selfsupporting target
$^{159}$Er
$^{158}$Er (4→2) 335.7
$^{159}$Er
$^{158}$Er (6→4)
443.8
$^{158}$Er (8→6)
523.8
$\beta^+$
90° Lead backed target
Counts x 10$^3$
Energy (keV)
150
200
300
400
500
0
1
2
3
4
5
XBL696-3008

Fig. 1.

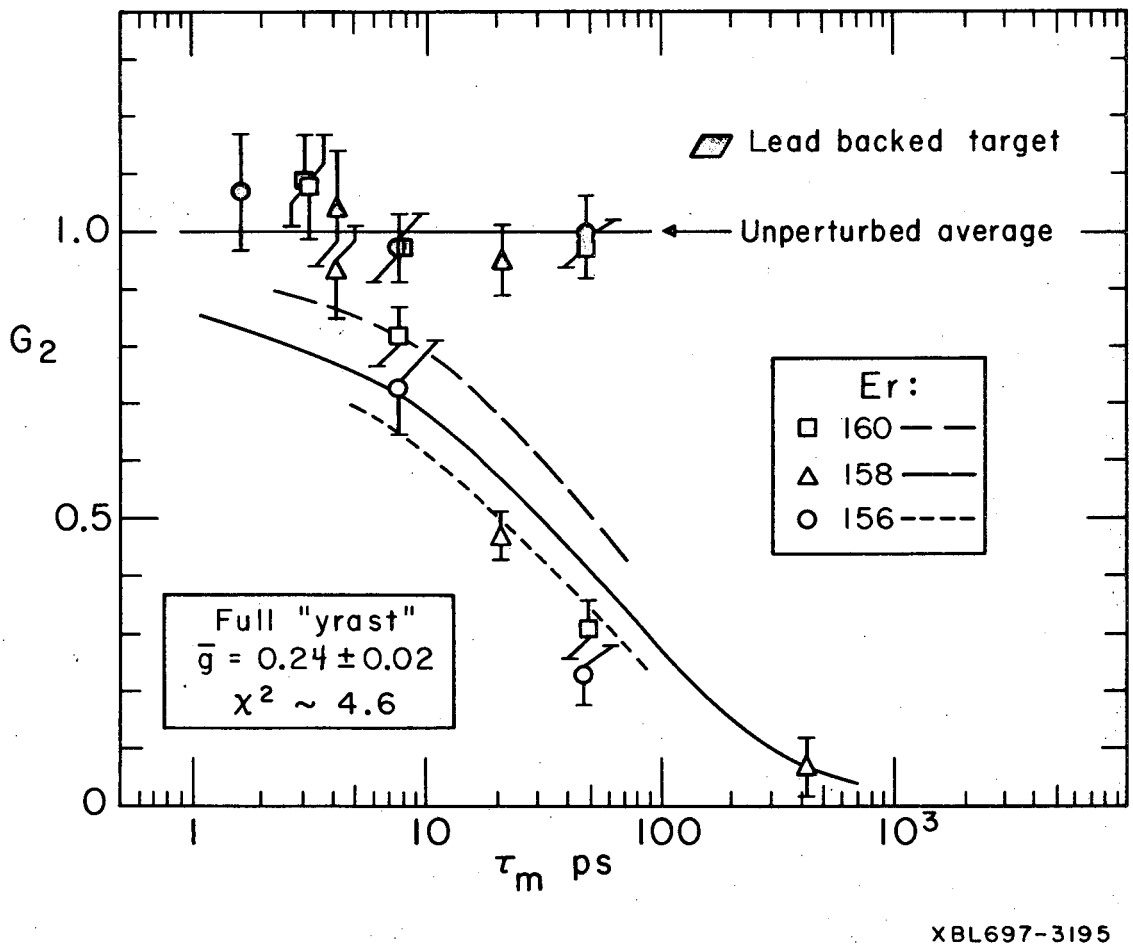
Lead backed target
Unperturbed average
1.0
0.5
0
$G_2$
Er:
160
158
156
Full "yrast"
$\bar{g}$ = 0.24 ± 0.02
$\chi^2$ ~ 4.6
1
10
100
$10^3$
$\tau_m$ ps
XBL697-3195

Fig. 2.

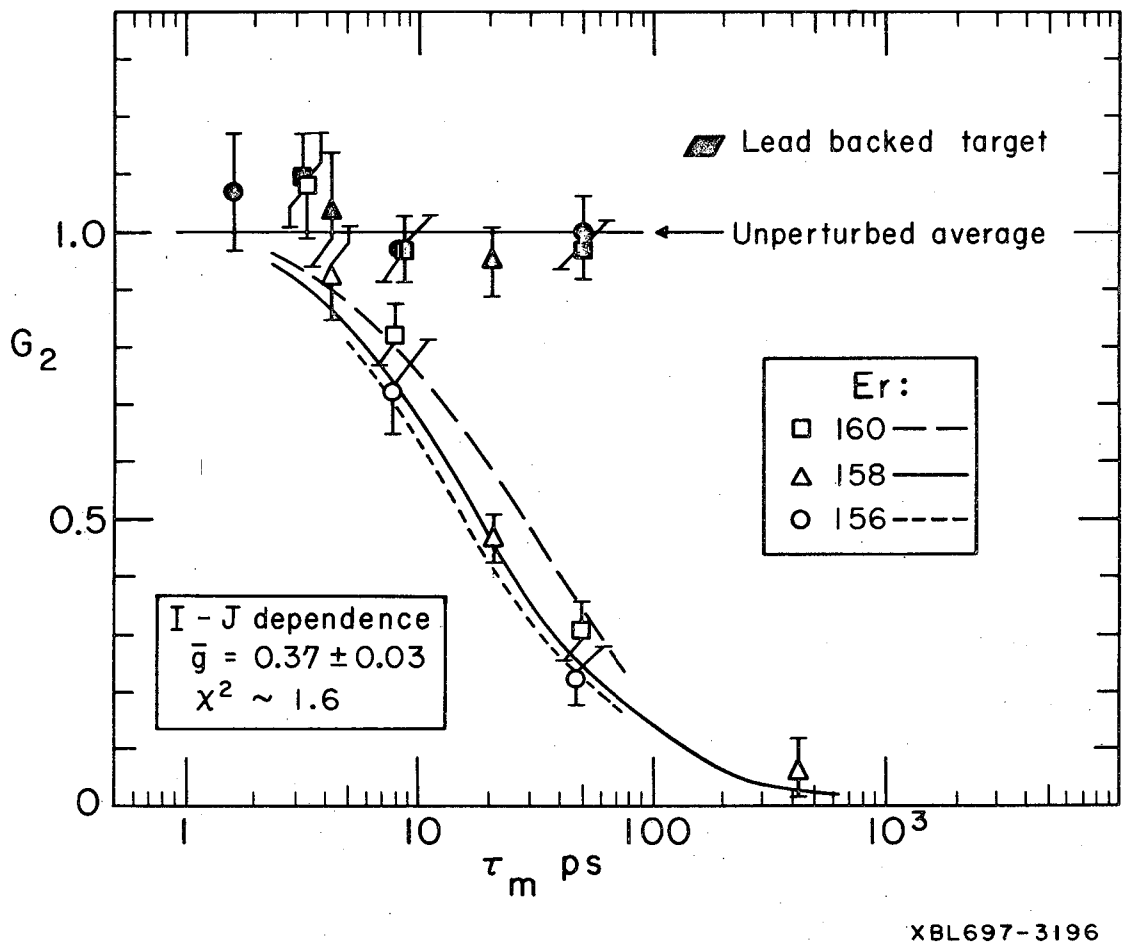
Lead backed target
Unperturbed average
1.0
0.5
0
$G_2$
Er:
160
158
156
I - J dependence
$\bar{g}$ = 0.37 ± 0.03
$\chi^2$ ~ 1.6
1
10
100
$10^3$
$\tau_m$ ps
XBL697-3196

Fig. 3.

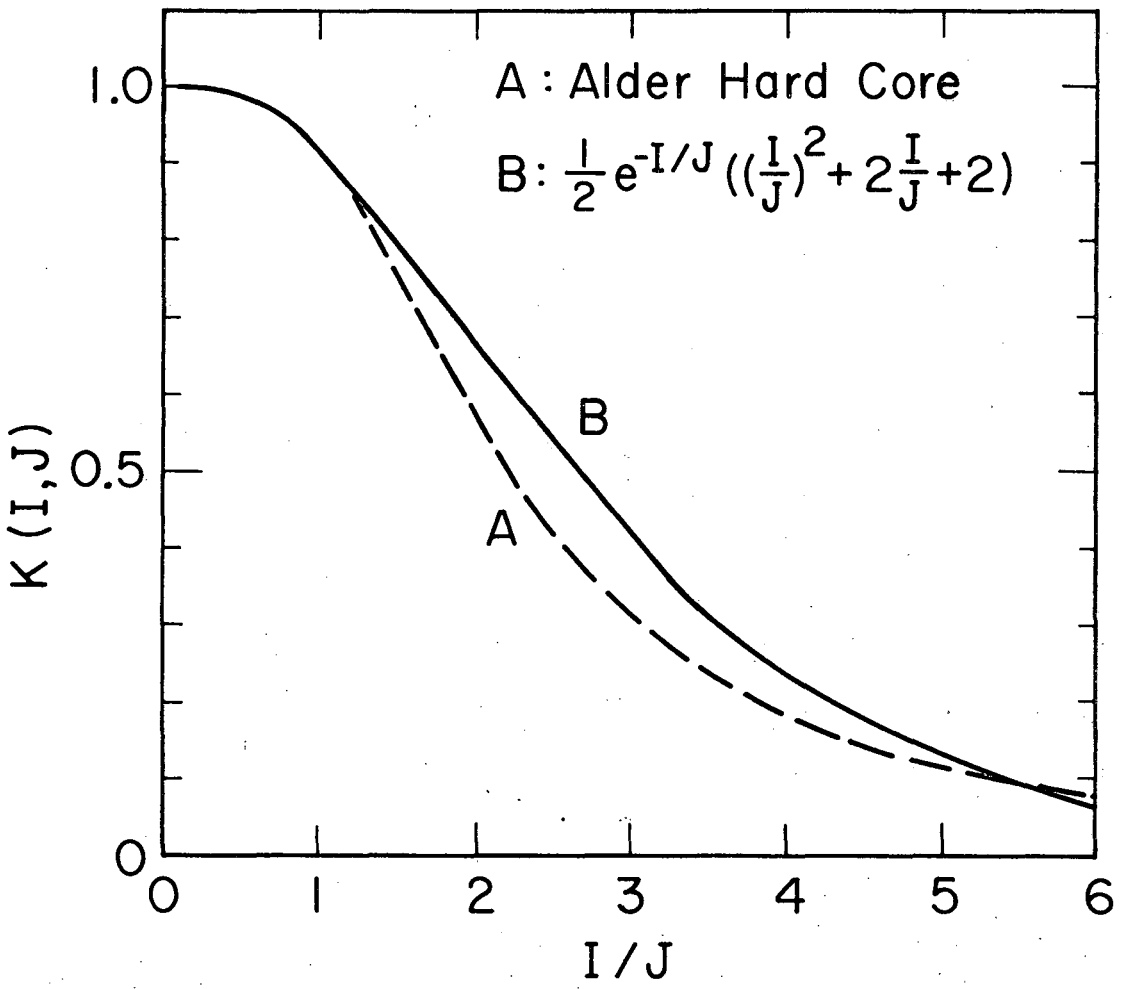


XBL696-3011

Fig. 4.

LEGAL NOTICE

*This report was prepared as an account of Government sponsored work. Neither the United States, nor the Commission, nor any person acting on behalf of the Commission:*

*A. Makes any warranty or representation, expressed or implied, with respect to the accuracy, completeness, or usefulness of the information contained in this report, or that the use of any information, apparatus, method, or process disclosed in this report may not infringe privately owned rights; or*

*B. Assumes any liabilities with respect to the use of, or for damages resulting from the use of any information, apparatus, method, or process disclosed in this report.*

*As used in the above, "person acting on behalf of the Commission" includes any employee or contractor of the Commission, or employee of such contractor, to the extent that such employee or contractor of the Commission, or employee of such contractor prepares, disseminates, or provides access to, any information pursuant to his employment or contract with the Commission, or his employment with such contractor.*

*TECHNICAL INFORMATION DIVISION*
*LAWRENCE RADIATION LABORATORY*
*UNIVERSITY OF CALIFORNIA*
*BERKELEY, CALIFORNIA 94720*